IOP Conf. Series: Journal of Physics: Conf. Series **1263** (2019) 012007 doi:10.1088/1742-6596/1263/1/012007

Introduction to Black Holes

Jutta Kunz

Institut für Physik, Universität Oldenburg, D-26111 Oldenburg, Germany

E-mail: jutta.kunz@uni-oldenburg.de

Abstract. In these lectures an introduction to black holes in general relativity is presented. First the Schwarzschild black hole and its properties are discussed by studying the geodesics of light and matter. Several coordinate systems are introduced, and the maximal analytic extension of the Schwarzschild solution is obtained, including a white hole, a second universe, and a non-traversable wormhole. Subsequently the properties of the rotating Kerr black hole are discussed. These include, in particular, the ring singularity, the horizons, frame dragging and the ergoregion. As an interesting astrophysical application the photon region and the black hole shadow are addressed.

1. Introduction

The standard model of particle physics [1] is based on Einstein's theory of special relativity and on quantum theory. Combined to relativistic quantum field theory these theories describe the electroweak and the strong interactions in terms of gauge theories. The fundamental particles then interact via the exchange of gauge bosons and get their masses via the Higgs mechanism. Gravity, however, cannot be included in this highly successful theoretical framework in a straightforward way.

After having proposed special relativity in 1905, Einstein presented in 1915 his new theory of gravity, general relativity (GR) (see e.g. [2, 3, 4, 5, 6, 7, 8]). In special relativity space and time had already been united to form a 4-dimensional space-time, referred to as Minkowski space-time. No longer were space and time simply arenas, where events would unfold as in Newton's absolute space and absolute time. Now time would run differently in different coordinate systems, since it would depend on the state of motion of the observer, and the notion of simultaneity would lose its absolute meaning. Likewise the measurement of length or distance would become relative, depending on the state of motion of the observer.

The formalism of special relativity classifies all physical quantities in terms of their transformation properties under Lorentz transformations. Thus there are scalars, which are invariant under these transformations, there are 4-vectors, and there are tensors of higher rank. If some physical law is expressed in terms of such tensors, then this physical law will have the same form in any inertial frame, and the theory is called covariant.

In his attempt to formulate an adequate relativistic theory of gravity Einstein had to go beyond special relativity. He then invoked the formalism of (pseudo-)Riemannian geometry in order to describe gravity via the curvature of space-time. Here a key ingredient is the metric tensor $g_{\mu\nu}$, which defines the line element of a space-time

$$ds^2 = g_{\mu\nu} dx^\mu dx^\nu, \tag{1}$$

where the components $g_{\mu\nu}$ are functions of the space-time coordinates. According to the equivalence principle, one can always choose a reference frame, which locally looks like Minkowski space-time.

From a physical point of view the metric $g_{\mu\nu}$ contains the gravitational potentials. Since the metric is a symmetric tensor there are 10 independent such potentials, in general, in 4 space-time dimensions. The Newtonian potential is recovered from the time-time component of the metric g_{00} in the Newtonian limit of weak fields. In Newtonian theory the gravitational force corresponds to the gradient of the potential. Similarly, in GR the gravitational forces are described by the derivatives of the metric – in the form of the Christoffel symbols (or affine connection) $\Gamma^{\mu}_{\nu\lambda}$. Clearly, the $\Gamma^{\mu}_{\nu\lambda}$ arise in the derivation of the equations of motion of particles and light.

These equations governing the motion of particles and light in a given space-time are called the geodesics equations

$$\frac{d^2x^\gamma}{du^2} + \Gamma^{\gamma}_{\kappa\lambda}\frac{dx^\kappa}{du}\frac{dx^\lambda}{du} = 0, \tag{2}$$

where u is a so-called affine parameter along the curve. The motion of massive particles follows timelike curves, and the affine parameter can be chosen to be the proper time of the particle. The motion of massless particles follows lightlike curves. As in Special Relativity (SR) massive particles can only travel within the lightcone, and the lightcone bounds all causal influence. However, the shape and orientation of the lightcone will depend on the space-time, and we will investigate the lightcones in order to better understand the black hole space-times.

Another key ingredient for the description of gravity in GR is the Riemann curvature tensor $R_{\mu\nu\lambda\kappa}$, which specifies the curvature of space-time. The Riemann curvature tensor can be seen to arise in various ways and make the effects of the curvature of space-time visible. For instance, when one considers geodesics in a curved space-time, these geodesics will approach each other or recede from one another depending on the curvature of space-time. In a flat space-time initially parallel geodesics would always stay parallel. Then in a flat space-time the Riemann curvature tensor vanishes identically. From a physical point of view, we can interpret the components of the curvature tensor to describe the tidal forces.

Mathematically, the curvature tensor is obtained from derivatives and products of the Christoffel symbols. In fact, it is formed from the metric and its first and second derivatives, such that it is linear in the second derivatives and quadratic in the first derivatives. The Einstein tensor $G_{\mu\nu}$ is then obtained from the curvature tensor, by contracting indices, leading to the Ricci tensor $R_{\mu\nu}$ and the curvature scalar R. The Einstein tensor represents the left hand side of the celebrated Einstein equations

$$G_{\mu\nu} = R_{\mu\nu} - \frac{1}{2}g_{\mu\nu}R = \frac{8\pi G}{c^4}T_{\mu\nu}. \tag{3}$$

On the right hand side, G is Newton's gravitational constant, c is the velocity of light, and $T_{\mu\nu}$ is the stress-energy tensor of the respective matter distribution, that sources the gravitational field and thus the curvature of space-time.

The Einstein equations represent a set of non-linear second order partial differential equations. They are covariant, and thus they are form invariant under general coordinate transformations. They are constructed from tensors, i.e., mathematical objects, that possess particular transformation properties under general coordinate transformations. As pointedly expressed by Wheeler [3], it is the matter, which determines the curvature of space-time, and it is the curvature of space-time, which determines the motion of particles and light in this space-time.

In weak gravitational fields the Newtonian limit is recovered, while post-Newtonian corrections reproduce the correct perihelion shift of Mercury and bending of light. Strong gravitational fields are encountered in the vicinity of highly compact astrophysical objects such as neutron stars and black holes, as visualized in the artist concept of a black hole environment shown in figure 1. In the following black holes and their properties will be discussed, starting with the Schwarzschild black holes and then including rotation.

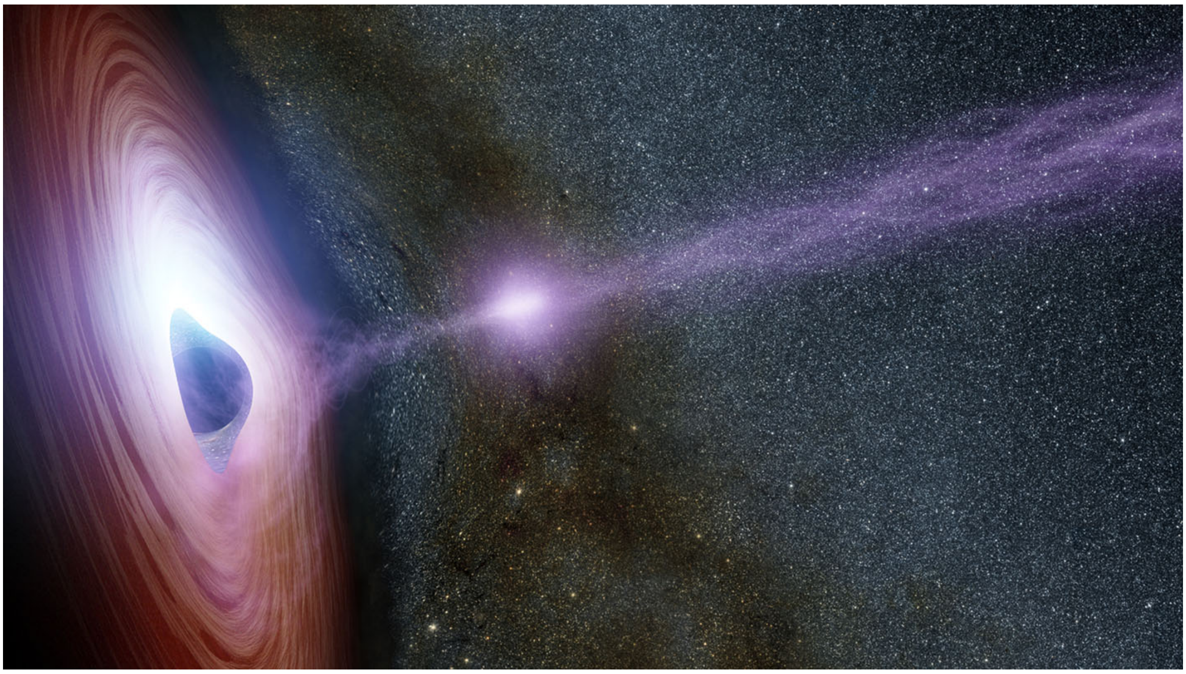

Figure 1. Black hole environment. Image credit: NASA/JPL-Caltech.

2. Schwarzschild black holes

Shortly after Einstein had formulated GR a first exact solution was found by Schwarzschild [9]. This spherically symmetric solution describes the space-time outside a star, and represents a good approximation for the space-time of our solar system. But the Schwarzschild solution also describes a static spherically symmetric black hole, i.e., the simplest type of a black hole.

2.1. Metric

By specifying a set of coordinates, the Schwarzschild time coordinate t, the Schwarzschild radial coordinate r, and the angular coordinates θ and ϕ, it is straigtforward to obtain the metric functions as a solution of the vacuum Einstein equations. The Schwarzschild metric then reads in geometric units ($G = c = 1$)

$$ds^2 = -\left(1 - \frac{2m}{r}\right) dt^2 + \left(1 - \frac{2m}{r}\right)^{-1} dr^2 + r^2 \left(d\theta^2 + \sin^2\theta d\phi^2\right), \tag{4}$$

where m corresponds to the mass of the black hole. If we were to put the mass equal to zero, the metric would simply correspond to Minkowski space-time in spherical coordinates. The angular coordinates θ and ϕ retain their usual meaning also in the Schwarzschild space-time. The radial coordinate r retains only part of its usual meaning, namely the circumference of a circle around the origin at the radial coordinate r is still given by $2\pi r$ and the surface of a sphere by $4\pi r^2$. However, r no longer describes the proper distance to the origin.

While the Schwarzschild metric looks rather simple, inspection of the metric coefficients shows, that there are several singularities which need to be addressed. Besides the well-known coordinate singularities present in spherical coordinates ($\theta = 0, \pi$), there are further singularities: $r = 2m$ and $r = 0$. At the surface $r = 2m$ the metric coefficient g_{00} is zero, while the metric coefficient g_{rr} diverges, or, denoting the inverse metric tensor by $g^{\mu\nu}$, its component g^{rr} is zero here. The surface $r = 2m$ is called the Schwarzschild radius, and we will see, that it corresponds to the event horizon of the Schwarzschild black hole. Thus it represents another coordinate singularity. For stars this coordinate singularity is not encountered, since it would reside far in the interior, where the vacuum Einstein equations would not hold any more, because of the presence of matter. For the singularity at $r = 0$, however, we find a divergence of the curvature, signaling that $r = 0$ does correspond to a physical singularity. In its vicinity the equations of GR will no longer hold, and a quantum theory of gravity should be invoked (see e.g. [10]).

2.2. Geodesics

To understand the physical meaning of the Schwarzschild solution and the Schwarzschild radius let us consider geodesics in this space-time, beginning with the radial null geodesics, i.e., the paths of light going radially inwards or outwards. We obtain these geodesics in a straightforward and fast way from the Lagrangian formalism. We read off the Lagrangian L^* directly from the metric

$$-L^* = \epsilon = \left(1 - \frac{2m}{r}\right)\dot{t}^2 - \left(1 - \frac{2m}{r}\right)^{-1}\dot{r}^2 - r^2\left(\dot{\theta}^2 + \sin^2\theta\dot{\phi}^2\right), \tag{5}$$

where the differentiation with respect to the affine parameter u is denoted by a dot.

To obtain radial geodesics, we set θ and φ to be constant, and for null geodesics we must set ϵ to zero, as well, since $ds = 0$ for light. We immediately read off the equation for the cyclic coordinate t, associated with energy conservation

$$\left(1 - \frac{2m}{r}\right)\dot{t} = E. \tag{6}$$

To obtain an equation for the radial coordinate we do not derive the Lagrange equation. Instead we simply take the Lagrangian, which corresponds to a first order equation

$$0 = \left(1 - \frac{2m}{r}\right)\dot{t}^2 - \left(1 - \frac{2m}{r}\right)^{-1}\dot{r}^2. \tag{7}$$

The resulting differential equation

$$\dot{r} = \pm E = \pm\left(1 - \frac{2m}{r}\right)\dot{t}, \tag{8}$$

and can be easily integrated to yield

$$t = \pm(r + 2m\ln|r - 2m| \ + \mathrm{const}) \tag{9}$$

We refer to the solutions with the $+$ sign as outgoing radial null geodesics, since in the region I, i.e., for $r > 2m$, the radial coordinate increases with increasing time t. Far from the Schwarzschild radius, i.e., for $r \to \infty$, the metric tends to the Minkowski metric. Therefore we say that the metric is asymptotically flat. The time coordinate t can therefore be interpreted as the proper time of an asymptotic static observer.

Analogously, we refer to the solutions with the $-$ sign as ingoing radial null geodesics, since for $r > 2m$, the radial coordinate decreases with increasing time t. However, as $r \to 2m$ a divergence arises. With respect to the Schwarzschild coordinate time t the Schwarzschild radius is only reached in the limit $t \to \infty$. Clearly the Schwarzschild coordinates are thus problematic. This divergence of the Schwarzschild time coordinate at the Schwarzschild radius has prompted the old name *frozen star* for the Schwarzschild solution [11, 12].

On the other hand, we can consider a radially infalling massive particle and ask, how long does such a particle need to reach $r = 2m$ or $r = 0$. We start by measuring the proper time τ of the particle. The only change in the above set of equations concerns ϵ, which must now be set to $\epsilon = 1$. Choosing $E = 1$ to simplify expressions, we find

$$\tau - \tau_0 = -\frac{1}{\sqrt{2m}}\frac{2}{3}\left(r^{3/2} - r_0^{3/2}\right) = +\frac{2}{3\sqrt{2m}}\left(r_0^{3/2} - r^{3/2}\right), \tag{10}$$

for a particle that starts at $r_0 > 2m$ at time τ_0. Thus the particle needs a finite proper time to first reach the Schwarzschild radius and then reach the central singularity. Moreover, nothing special appears to happen at the Schwarzschild radius.

If, however, we calculate with respect to the coordinate time t, we find

$$t - t_0 = \frac{2}{3\sqrt{2m}}\left(r_0^{3/2} - r^{3/2} + 6mr_0^{1/2} - 6mr^{1/2}\right) + 2m\ln\frac{\left[r^{1/2} + (2m)^{1/2}\right]\left[r_0^{1/2} - (2m)^{1/2}\right]}{\left[r_0^{1/2} + (2m)^{1/2}\right]\left[r^{1/2} - (2m)^{1/2}\right]}. \tag{11}$$

Now we see, that the coordinate time diverges as $r \to 2m$, thus in the coordinate time the particle will reach $r = 2m$ only in the limit $t \to \infty$. No wonder that the surface $r = 2m$ had been called the Schwarzschild singularity for a long time. An illustration is given in figure 2.

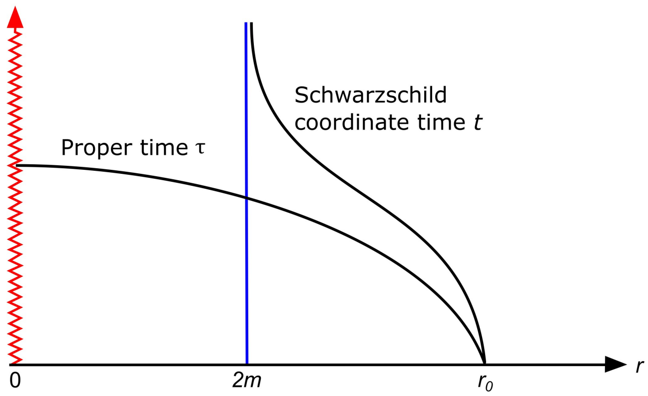

Figure 2. A radially infalling massive particle in the Schwarzschild space-time for the Schwarzschild coordinate time t and the proper time τ.

2.3. Redshift

Before we look for a better coordinate set, let us briefly halt and address the gravitational redshift. This can be done in Schwarzschild coordinates, since we are only interested in the region $r > 2m$. Let us consider light that is emitted from a surface with radial coordinate r and moving outwards. At the surface with radial coordinate r time is running more slowly than farther outwards, since

$$d\tau^2 = -g_{00}(r)dt^2 = \left(1 - \frac{2m}{r}\right)dt^2 \tag{12}$$

with a monotonically increasing coefficient $-g_{00}(r)$, and $-g_{00}(\infty) = 1$. Therefore the frequency decreases, as the wave moves outwards, in particular

$$\left(\frac{\nu_\infty}{\nu_r}\right)^2 = \frac{g_{00}(r)}{g_{00}(\infty)} = -g_{00}(r) = \left(\frac{\lambda_r}{\lambda_\infty}\right)^2, \tag{13}$$

while the wavelength increases. This leads to the gravitational redshift z

$$z = \frac{\lambda_\infty - \lambda_r}{\lambda_r}, \quad 1 + z = \frac{1}{\sqrt{-g_{00}}}, \tag{14}$$

with z diverging as $r \to 2m$. Thus at the Schwarzschild radius the gravitational redshift becomes infinite. We therefore refer to the Schwarzschild radius as an infinite redshift surface.

2.4. Event horizon

In order to gain further insight on the physical meaning of the Schwarzschild radius $r = 2m$ and to understand why this represents an event horizon, let us now change coordinates. Since we know, that the Schwarzschild time coordinate t is no longer valid in the region $r < 2m$, we certainly need a new time coordinate. Therefore let us introduce the so-called Eddington-Finkelstein time coordinate $\bar{t}$. We obtain this coordinate by transforming ingoing radial null geodesics into straight lines, i.e., the new Eddington-Finkelstein time coordinate is defined via

$$\bar{t} = ct + 2m \ln |r - 2m|. \tag{15}$$

Then the ingoing radial null geodesics are given by

$$\bar{t} = -r + \text{const}, \tag{16}$$

while at the same time the outgoing radial null geodesics become

$$\bar{t} = r + 2 \cdot 2m \ln |r - 2m| + \text{const}. \tag{17}$$

These null geodesics are illustrated in figure 3. We see that the light cones in region I, where $r > 2m$, open to both sides. A particle is free to move towards the black hole or away from it. The light cones far away from the black hole open under the usual 45° to both sides, while closer to the black hole, the light cones narrow and tilt somewhat towards the black hole. Most importantly, however, we realize why the Schwarzschild radius corresponds to an event horizon: at $r = 2m$ the right hand side of the light cones is vertical, while the remainder of the lightcone points inwards. In region II, where $r < 2m$, the lightcones then point always fully inwards. Thus any object inside this region has to hit the singularity in a finite proper time. Consequently any object will reach the singularity, once it has crossed the event horizon, and even light cannot escape. Moreover, observers outside the event horizon cannot receive any information from the interior region, thus the event horizon represents a boundary beyond which nothing can be known in the universe outside.

2.5. Collapse

Now that we have a new set of coordinates, we can, in principle, describe gravitational collapse. Let us simply consider the collapse of a star as illustrated in figure 4. The coordinates represent the radial Schwarzschild coordinate r and the new time coordinate $\bar{t}$. A hypothetical observer on the surface of the star is sending signals radially outwards in regular time intervals. As the surface shrinks, the star gets more compact, and the signals take longer and longer to reach a second observer far from the collapsing star. The signals get also more and more redshifted during the collapse. At a certain point in time, the surface of the star crosses the event horizon $r = 2m$. No signal emitted beyond that point will be received in the outside universe.

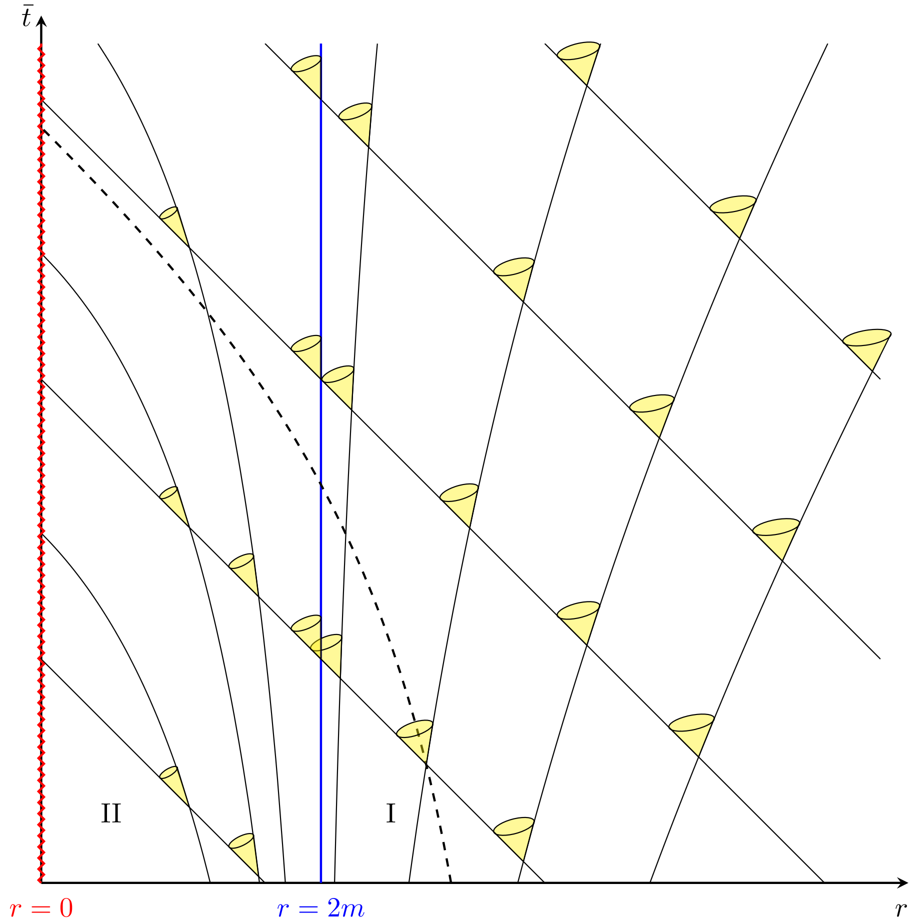

Figure 3. Schwarzschild space-time in Eddington-Finkelstein coordinates: $\bar{t}$, r, Eqs. (16)-(17).

2.6. Tidal forces

When a set of particles approaches a black hole, it is subject to tidal forces, since the gravitational forces become stronger towards the event horizon. Assuming all particles to follow geodesics, their angular distance will decrease, since they all are attracted towards the center. Moreover, their radial distance will increase, since the particles closer to the black hole will be accelerated more strongly, so the distribution of particles will be squeezed vertically to the direction of motion and stretched in the direction of motion. The stretching corresponds to a tension, while the squeezing corresponds to a pressure.

We refer to these forces as the tidal forces. An illustration is shown in figure 5. As discussed above, the tidal forces are obtained from the curvature tensor. They are proportial to the mass of the black hole and inversely proportional to the 3rd power of the radial coordinate r. Tidal forces are always present in a gravitational field, since there is no uniform gravitational field. Since these tidal forces will become extremely strong in the vicinity of the horizon of a not too big black hole, any object approaching the event horizon will be torn to pieces. One therefore often refers to the action of the tidal forces as *spaghettification*.

*2.7. Sagittarius A**

Besides stellar black holes like Cygnus X-1 [13, 14], which have masses on the order of several to several tens of solar masses, there are supermassive black holes with millions and billions of

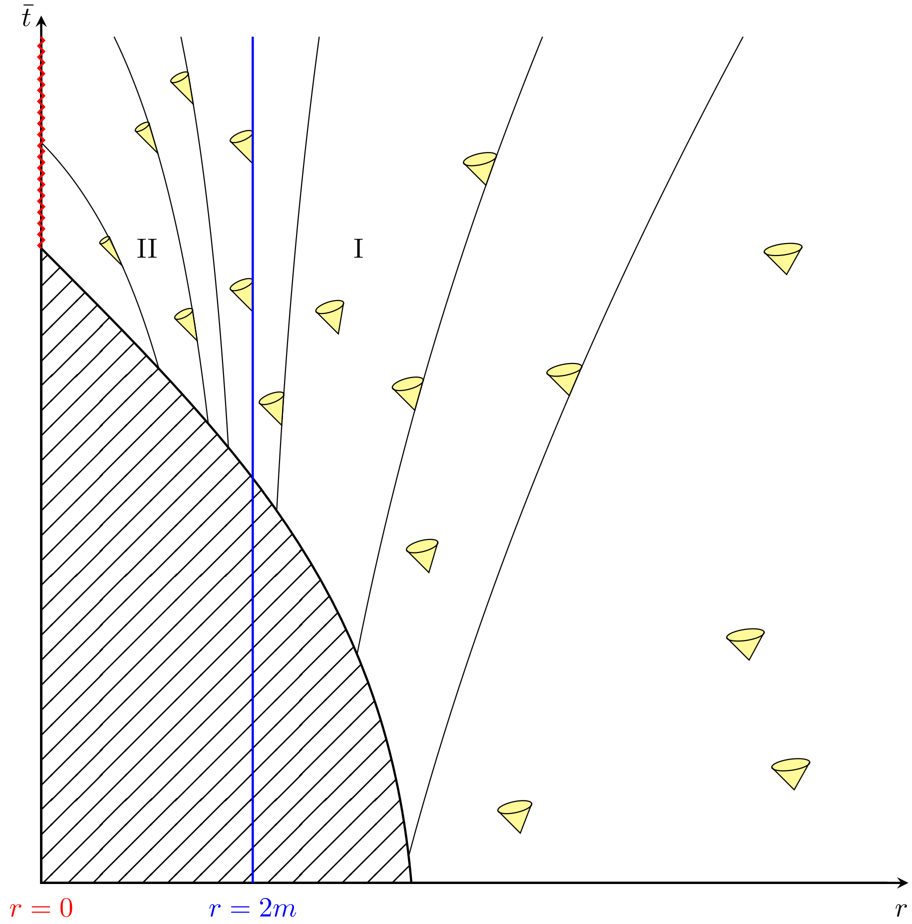

Figure 4. Collapse of a star.

solar masses, located at the galactic center of spiral and elliptic galaxies [15, 16]. Our Milky Way also has such a supermassive black hole sitting at its center, but only one of moderate size.

Since more than 20 years, the motion of giant stars around the Milky Ways supermassive black hole has been observed [17, 18, 19], leading to a mass estimate for this black hole of more than 4 million solar masses. The orbits of some of these stars are illustrated in figure 6. In particular, the star named $S2$ has fully completed its orbit during these years. Recently measurements of this star's motion allowed for a determination of the redshift at its closest approach and led to another success of GR [20].

2.8. White holes

Coming back to the Schwarzschild black hole we note that, interestingly, we can make another coordinate transformation,

$$ct^* = ct - 2m \ln |r - 2m|, \tag{18}$$

where we make the outgoing radial null geodesics straight lines

$$t^* = r + \text{const}, \tag{19}$$

while the ingoing radial null geodesics become

$$t^* = -r - 2 \cdot 2m \ln |r - 2m| + \text{const}. \tag{20}$$

IOP Conf. Series: Journal of Physics: Conf. Series **1263** (2019) 012007 doi:10.1088/1742-6596/1263/1/012007

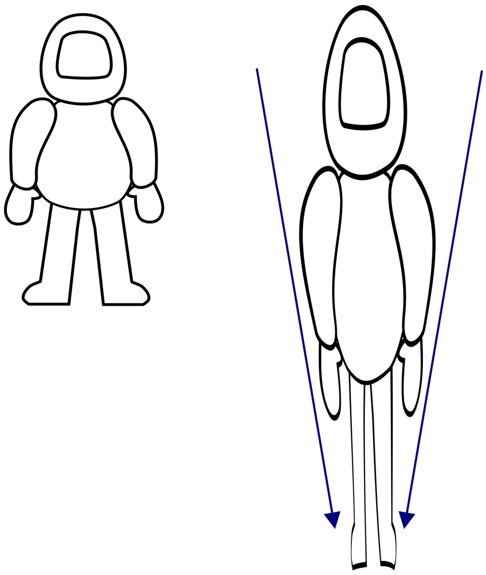

Figure 5. Tidal forces

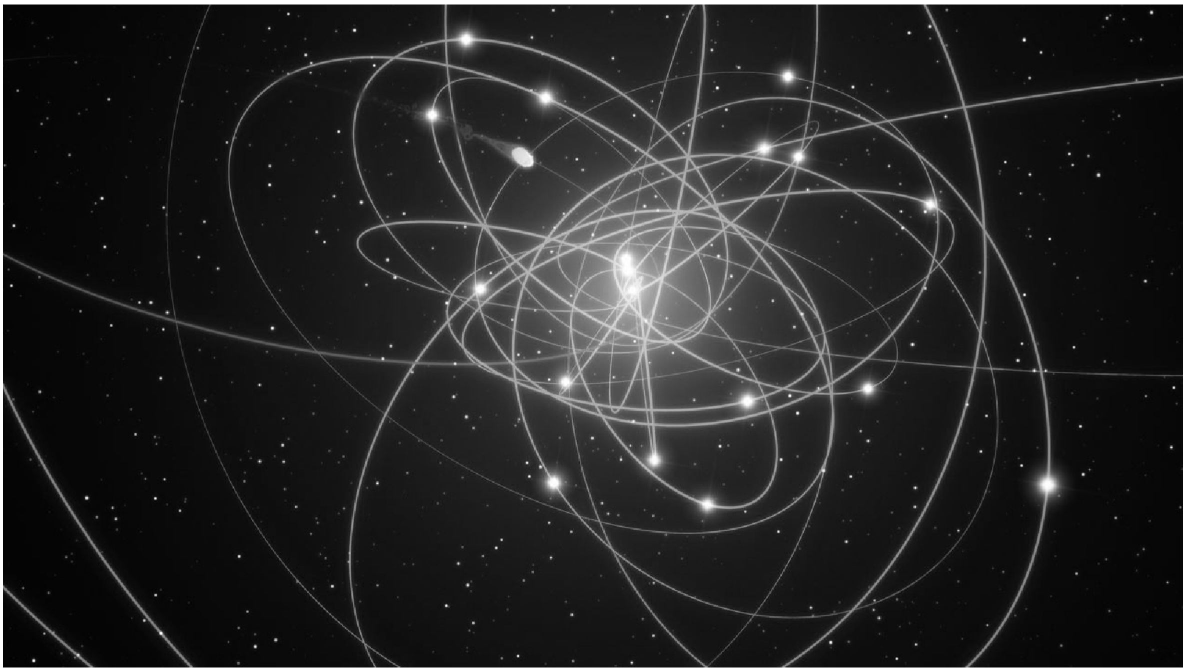

Figure 6. Motion of stars around Sagittarius A*. Image credit: ESO.

These coordinates are illustrated in figure 7. Here we now seem to have the reverse situation. Nothing can penetrate from region I into region II, since the light cones point outwards, away from the singularity, and their left hand side is now vertical at the Schwarzschild radius. In that case, the region $r \leq 2m$ is referred to as a white hole. Nothing can enter a white hole from the universe outside, i.e., the region $r > 2m$, but the horizon $r = 2m$ is traversable from the inside towards the outside. It is again a semipermeable membrane, but now in the other direction.

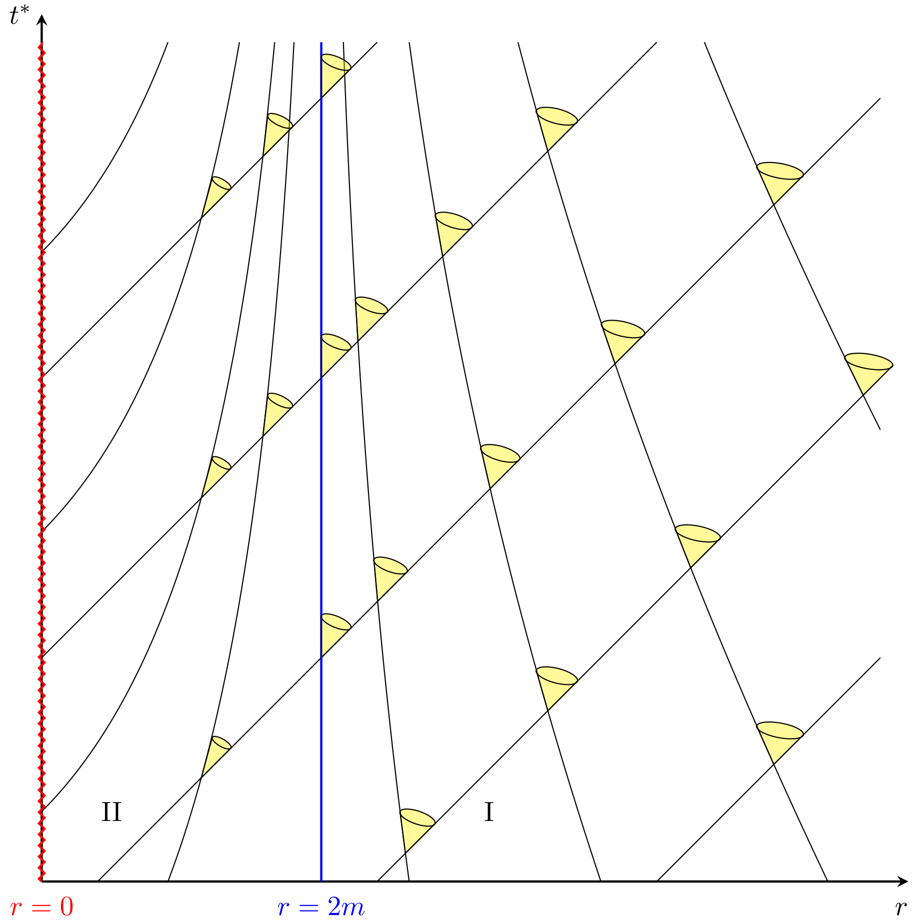

Figure 7. White hole

2.9. Extended space-time

Let us recap: there is an exterior region, outside the Schwarzschild radius, and there are two different interior regions, corresponding to a black hole and a white hole. Would it be possible that there is even more like, for instance, another exterior region?

We can answer this question by making further coordinate transformations, following Kruskal and Szekeres. Let us start from the Eddington-Finkelstein double null coordinates

$$v = \bar{t} + r, \quad w = t^* - r, \tag{21}$$

which are obtained from the two new Eddington-Finkelstein time coordinates $\bar{t}$ and t^* and the Schwarzschild radial coordinate r. The null coordinates v and w are somewhat analogous to lightcone coordinates in Minkowski space-time.

Next we consider combinations of these null coordinates. These lead to a new radial coordinate, the tortoise coordinate x, and back to the Schwarzschild time coordinate

$$x = \frac{1}{2}(v - w) = r + 2m \ln |r - 2m|, \quad t = \frac{1}{2}(v + w). \tag{22}$$

The name tortoise coordinate can be associated with Zeno's paradox on the race between Achilles and the tortoise, since the tortoise coordinate x approaches minus infinity, as the Schwarzschild coordinate r approaches the Schwarzschild radius. Interestingly, the relevant (2-dimensional) part of the metric (leaving out the usual angular part) now becomes

$$ds^2_{(2)} = -\left(1 - \frac{2m}{r}\right)\left(dt^2 - dx^2\right), \tag{23}$$

i.e., it exhibits the same causal structure as a 2-dimensional Minkowski space-time, where the light cones open under 45°.

While this latter fact is very nice, the metric is still problematic, since the conformal factor, as the factor in brackets is called, vanishes at the horizon. Moreover, the metric again contains the deficient Schwarzschild time t. Here the following simple coordinate transformation will help. We introduce new double null coordinates v' and w', that are associated with the new coordinates

$$x' = \frac{1}{2}\left(v' - w'\right), \quad t' = \frac{1}{2}\left(v' + w'\right), \tag{24}$$

such that the new metric reads

$$ds^2_{(2)} = -F^2(t', x')\left(dt'^2 - dx'^2\right). \tag{25}$$

The coordinate transformations $v'(v)$ and $w'(w)$ are then chosen to make the metric regular, and the final result for the metric reads

$$ds^2 = -\frac{16m^2}{r}\exp\left(-\frac{r}{2m}\right)\left(dt'^2 - dx'^2\right) + r^2\left(d\theta^2 + \sin^2\theta d\phi^2\right), \tag{26}$$

where different transformations are needed for the different regions. In particular, since there is no reason to restrict the coordinate x' to be positive, there emerges a second asymptotically flat region, that is completely analogous to the first asymptotically flat region. The full space-time is illustrated in figure 8.

In the figure the horizons correspond to the diagonals $r = 2m$. The black hole resides in the upper region II. It is bounded by the future singularity $r = 0$. The white hole resides in the lower region II'. It is bounded by the past singularity $r = 0$. The universe I exterior to the black hole and the white hole has a mirror universe I', which is completely analogous, but resides at negative x'. Except for the horizons, the curves of constant r represent hyperbolae. For $r > 2m$ these reside in the regions I and I', while for $r < 2m$ they reside in the regions II and II'. Curves of constant t represent straight lines.

2.10. Wormhole

The causal structure can directly be read off the diagram, since the light cones have 45° opening angles on each side. This makes it very simple to see what motion is possible or impossible. In particular, the causal boundaries presented by the horizons are obvious. Moreover, we see that the space-time harbours a wormhole, the Einstein-Rosen bridge. However, the wormhole is not traversable. One cannot reach region I' from region I or vice versa on a timelike or lightlike path. Only by travelling faster than light could one traverse from one asymptotically flat region to the other. An illustration of such a wormhole is shown in figure 9.

2.11. Penrose diagram

Before we leave the Schwarzschild space-time, we would like to make another transformation, which gives us the possibility to bring infininity into a finite region, and thus to illustrate the full extended space-time. For this purpose we compactify the coordinates, using for instance the arctan function, which maps spatial infinity to a finite value. The resulting diagram is called a Penrose diagram, and it retains the causal structure with light cones possessing 45° opening angles. The Penrose diagram of the extended Schwarzschild solution is exhibited in figure 10.

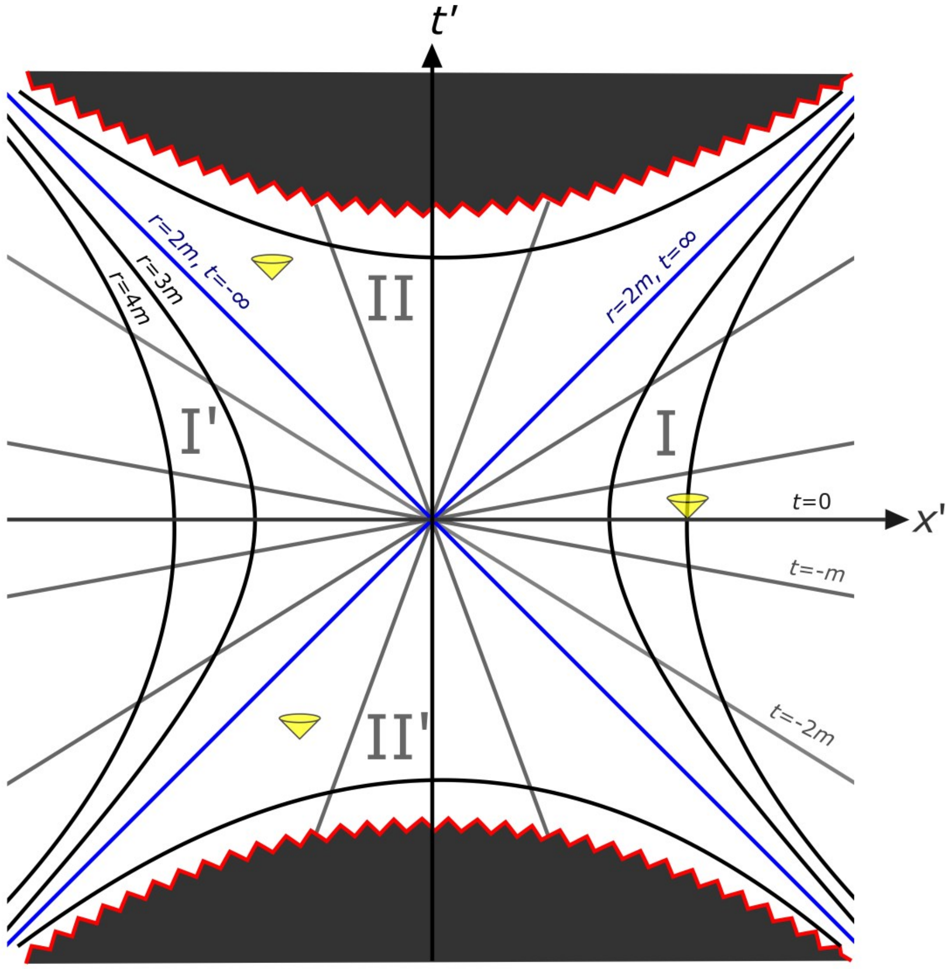

Figure 8. Extended Schwarzschild space-time in Kruskal-Szekeres coordinates t', x'.

3. Rotating black holes

Now we will address rotating black holes and their maybe even more bizarre properties. While the Schwarzschild black hole solutions had been found immediately after GR had been formulated, it took almost 50 years until their rotating generalization was found by Kerr [21, 22, 23]. Consequently, after their discoverer, these rotating black holes are called Kerr black holes. Since astrophysical black holes are expected to typically rotate, the Kerr solution is considered to be of high astrophysical relevance.

3.1. Metric

Let us begin by inspecting the metric of the Kerr black hole given in so-called Boyer-Lindquist coordinates. The metric then reads

$$ds^2 = -\frac{\Delta}{\rho^2}\left(dt - a\sin^2\theta d\phi\right)^2 + \frac{\sin^2\theta}{\rho^2}\left(\left(r^2+a^2\right)d\phi - adt\right)^2 + \frac{\rho^2}{\Delta}dr^2 + \rho^2 d\theta^2 \quad (27)$$

with

$$\Delta = r^2 - 2mr + a^2, \quad \rho^2 = r^2 + a^2\cos^2\theta. \quad (28)$$

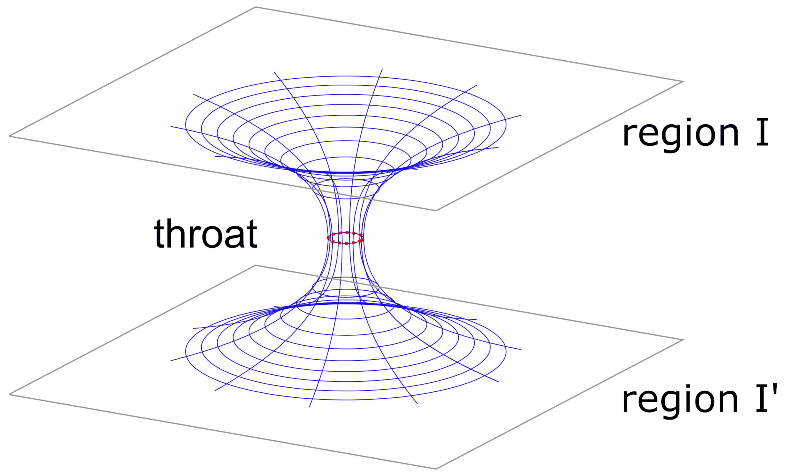

Figure 9. Embedding diagram of a wormhole.

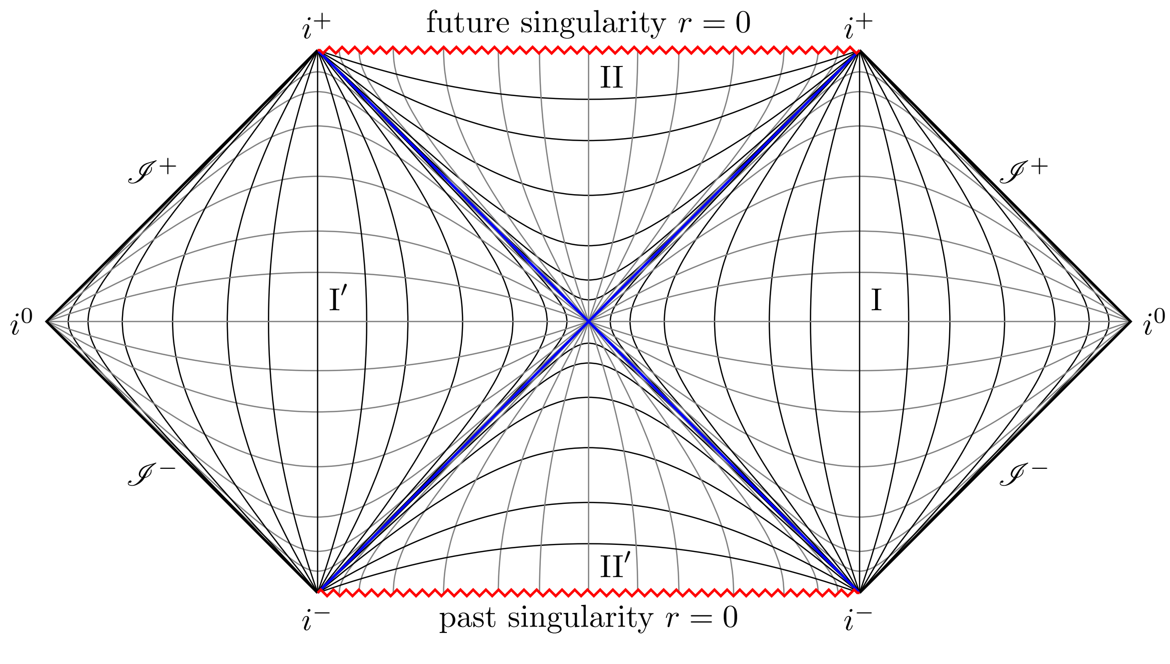

Figure 10. Penrose diagram of the extended Schwarzschild space-time.

Clearly, the metric is axially symmetric and stationary. There is no explicit dependence of the metric functions on the azimuthal angle ϕ and on the time coordinate t. There is, however, now a new non-trivial dependence of the metric functions on the polar angle θ, while a dependence on the radial coordinate r is, of course, retained.

The Kerr metric depends on two constants, m and a. When $a \to 0$, the Schwarzschild space-time is recovered. So it is natural to expect, that the constant m still specifies the mass of the black hole, while the constant a is associated with the rotation of the black hole. In fact, it turns out that the constant a describes the specific angular momentum of the black hole, $a = J/m$, when the angular momentum is denoted by J. We can convince ourselves that the cross term $dtd\phi$ signals rotation, since we obtain precisely such a cross term, when we make a coordinate transformation from a non-rotating coordinate system to a rotating one.

3.2. Ring singularity
Obviously, there are again singularities in the metric, which need to be considered. After noting the trivial coordinate singularity on the rotation axis associated with the angular coordinates, let us address the physical singularity associated with the divergence of the curvature in the central part of the black hole. Inspection shows that the physical singularity arises for

$$\rho^2 = r^2 + a^2 \cos^2\theta = 0. \tag{29}$$

This means, that two conditions must be satisfied,

$$r = 0 \quad \text{and} \quad \cos\theta = 0. \tag{30}$$

Thus the singularity is located in the equatorial plane at $r = 0$. This may look a bit surprising. Why should we specify $\cos\theta = 0$, when $r = 0$? The reason is our choice of coordinates. If we were to use a different set of coordinates, e.g., those used by Kerr when deriving the solution,

$$\begin{aligned} x &= r\sin\theta\cos\varphi + a\sin\theta\sin\varphi, \\ y &= r\sin\theta\sin\varphi - a\sin\theta\cos\varphi, \\ z &= r\cos\theta, \end{aligned} \tag{31}$$

we would realize immediately that $r = 0$ corresponds to a ring in the equatorial plane, $x^2 + y^2 = a^2$. Consequently, the physical singularity of the Kerr black hole is a ring singularity.

3.3. Infinite redshift surface
As we discussed above, when the metric coefficient g_{00} vanishes, this points to an infinite redshift surface. For Schwarzschild black holes, this hypersurface coincides with the horizon of the black hole, but for Kerr black holes this is no longer the case. Let us inspect where this infinite redshift surface is located by collecting the contributions to g_{00} in the metric and requiring g_{00} to be zero

$$g_{00} = -\frac{\Delta}{\rho^2} + \frac{\sin^2\theta}{\rho^2}a^2 = -\frac{r^2 - 2mr + a^2 - \sin^2\theta a^2}{\rho^2} = 0. \tag{32}$$

Interestingly we here find a quadratic equation and thus two hypersurfaces

$$r_{S_\pm} = m \pm \sqrt{m^2 - a^2\cos^2\theta}. \tag{33}$$

The physically most important one is the outer hypersurface r_{S_+}, since it does not only correspond to an infinite redshift surface, but it has other highly significant properties associated with the motion of particles and light in the exterior – and thus observable – space-time, as will be discussed below. The two hypersurfaces $r_{S_\pm}$ are illustrated in figure 11.

The two hypersurfaces $r_{S_\pm}$ are axially symmetric. At the equator $r_{S_+} = 2m$, while $r_{S_-} = 0$, i.e., r_{S_-} touches the ring singularity. At the poles $r_{S_+} = m + \sqrt{m^2 - a^2} < 2m$ while $r_{S_-} = m - \sqrt{m^2 - a^2} > 0$. In the limit $a \to 0$ the surface r_{S_+} agrees with the Schwarzschild horizon, whereas $r_{S_-} = 0$, i.e., it shrinks to a point, the point singularity.

IOP Conf. Series: Journal of Physics: Conf. Series **1263** (2019) 012007 doi:10.1088/1742-6596/1263/1/012007

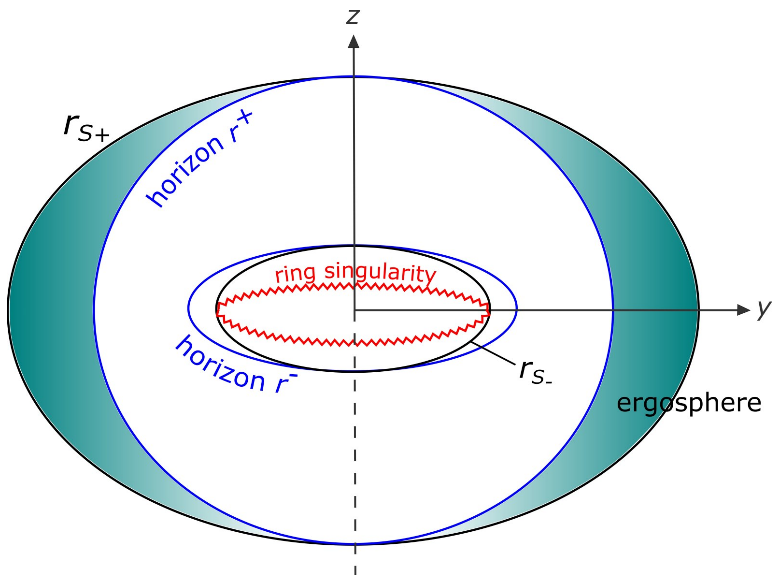

Figure 11. Sketch of various features of the Kerr space-time.

3.4. Horizons

We now expect that, as in the Schwarzschild space-time, the location of the event horizon will be determined by the hypersurface $g^{rr} = 0$

$$g_{rr} = \frac{\rho^2}{\Delta} \quad \Longrightarrow \quad g^{rr} = \frac{\Delta}{\rho^2}. \tag{34}$$

The condition $g^{rr} = 0$ again leads to a quadratic equation

$$\Delta = r^2 - 2mr + a^2 = 0, \tag{35}$$

which has the formal solutions

$$r_\pm = m \pm \sqrt{m^2 - a^2}. \tag{36}$$

The radial coordinate of the location of the black hole horizons should be a physical quantity in the sense that it corresponds to a real and not to an imaginary number. This means that we have to make a distinction of cases:

(i) two distinct horizons: $m > a$,

(ii) a degenerate horizon: $m = a$,

(iii) no horizon: $m < a$.

The physically most relevant case is the case (i) with two distinct horizons, an outer horizon r_+ and an inner horizon r_-. We will concentrate most of the discussion on this case. The case (ii) with a degenerate horizon, i.e., the two horizons coincide, $r_+ = r_-$, is said to describe an extremal black hole, since here the ratio of a/m and thus the angular momentum of the black hole for a given mass is maximal. Thus the angular momentum for a black hole of a given mass is bounded above. This bound is referred to as the Kerr bound, $J/m^2 = 1$. In the case (iii), however, there is no horizon any more, that could shield the ring singularity from the universe outside, therefore this case is referred to as representing a naked singularity. Such a naked singularity is abhorred by many scientists, and Penrose has formulated the cosmic censorship conjecture in order to ban such a beast from our universe [24, 25].

Let us now focus on case (i), where there are two horizons. The space-time then seems to consist of 3 regions

- I. $r_+ < r$, the exterior region outside the black hole,
- II. $r_- < r < r_+$, the region between the two horizons,
- III. $r < r_-$, the inner region around the singularity.

The horizons are also illustrated in figure 11, where we notice that on the rotational axis the horizons $r_\pm$ coincide with the respective hypersufaces $r_{S_\pm}$. Apart from these points on the axis, the outer horizon r_+ is located inside the infinite redshift surface r_{S_+}. The region between the surface r_{S_+} and the outer horizon r_+ is called the ergosphere.

The horizons are located at hypersurfaces specified by constant values of the radial Boyer-Lindquist coordinate r. One might therefore be tempted to think, that the spatial part of these surfaces would be spherical, i.e., that the horizons would correspond to geometric spheres. However, this is not the case. When one calculates, for instance, the circumference of the horizon at the equator, one finds

$$\int_0^{2\pi} \sqrt{g_{\phi\phi}} d\phi = \frac{r_+^2 + a^2}{r_+} \int_0^{2\pi} d\phi = 2\pi \frac{r_+^2 + a^2}{r_+}, \tag{37}$$

while one might have expected $2\pi r_+$. Likewise, when one calculates the surface of the horizon, one finds

$$A_{\rm H} = \int_0^{2\pi} \int_0^{\pi} \sqrt{g_{\theta\theta} g_{\phi\phi}} d\theta d\phi \bigg|_{r_+} = 4\pi \left(r_+^2 + a^2 \right), \tag{38}$$

which neither corresponds to the perhaps expected $4\pi r_+^2$, nor to the value that one would find by using the above circumferential radius of the equator. Clearly, the horizon is deformed. But this should not be too surprising, since we usually observe deformation, when an object is rotating, just think of the flattened Earth. This deformation of the horizon is also indicated in figure 11.

3.5. Geodesics

In order to convince ourselves that the hypersurfaces $r_\pm$ really correspond to horizons, let us again consider the light cones and see how they change, as we move towards the black hole from far away. Clearly, at large distances the light cones will be hardly squeezed or tilted, since the space-time is asymptotically flat. But the closer we get to the black hole, the stronger its presence will become manifest in the light cones. Let us therefore evaluate the null geodesics for the Kerr space-time.

The Lagrangian now reads

$$\mathcal{L}^* = -\frac{\Delta}{\rho^2} \left[\dot{t} - a \sin^2\theta \dot{\phi} \right]^2 + \frac{\sin^2\theta}{\rho^2} \left[(r^2 + a^2)\dot{\phi} - a\dot{t} \right]^2 + \frac{\rho^2}{\Delta} \dot{r}^2 + \rho^2 \dot{\theta}^2. \tag{39}$$

Obviously, the time coordinate t and the azimuthal angle coordinate ϕ are still cyclic coordinates, so there is conservation of energy E and angular momentum L for particles and light, and the Lagrangian itself is constant for their orbits. Thus there are already 3 constants of motion. If there were 4 constants of motion, the system of the equations of motion in the Kerr space-time would be fully integrable, and this is, indeed, the case, as shown by Carter [26], who obtained another constant of motion in his analysis, that is now named the Carter constant. This allows for a complete integration of the equations of motion in terms of explicit quadratures.

In order to construct the light cones, we must study the null geodesics, i.e., $\mathcal{L}^* = 0$. But whereas we considered radial null geodesics in the Schwarzschild space-time, we can no longer restrict to this case here, since the space-time itself is rotating. Therefore anything inside the space-time, be it matter or light, is dragged along in the direction of the rotation of space-time. We call this effect thus frame dragging. Before we discuss frame dragging further, let us look at the equations for the null geodesics, obtained from the above Lagrangian, by choosing θ to be constant for simplicity.

This leads to the set of equations

$$\frac{dt}{dr} = \pm \frac{r^2 + a^2}{\Delta}, \tag{40}$$

$$\frac{d\phi}{dr} = \pm \frac{a}{\Delta}. \tag{41}$$

For the outgoing null geodesics we choose the + sign, since the radial coordinate increases with time. Integration then gives

$$t = r + \left(m + \frac{m^2}{\sqrt{m^2 - a^2}} \right) \ln |r - r_+| + \left(m - \frac{m^2}{\sqrt{m^2 - a^2}} \right) \ln |r - r_-| + \text{const}, \tag{42}$$

$$\phi = \frac{a}{2\sqrt{m^2 - a^2}} \ln \left| \frac{r - r_+}{r - r_-} \right| + \text{const}. \tag{43}$$

The ingoing null geodesics are obtained with the $-$ sign, and thus we obtain analogous expressions but with opposite signs.

These geodesics immediately show, that the time coordinate t diverges at the horizon r_+. Likewise, there is a divergence at r_-. But not only the time coordinate diverges at the horizon. Also the azimuthal coordinate ϕ diverges for $r \to r_+$ (or $r \to r_-$). This is a new phenomenon as compared to the Schwarzschild space-time, where only the time coordinate did diverge, that is clearly due to the rotation of the space-time. Since such divergences indicate coordinate singularities, let us look for coordinate transformations, that will remove these. In the new coordinates the interpretation of r_+ as the event horizon of the black hole will immediately become clear.

3.6. Eddington-Finkelstein coordinates

Let us introduce the coordinate transformation

$$d\bar{t} = dt + \frac{2mr}{\Delta} dr, \quad d\bar{\phi} = d\phi + \frac{a}{\Delta} dr. \tag{44}$$

Then ingoing null geodesics satisfy

$$d\bar{t} = -dr, \quad d\bar{\phi} = 0, \tag{45}$$

i.e., ingoing null geodesics become straight lines. The ingoing and outgoing null geodesics are illustrated in figure 12.

In these new coordinates we see, that the right hand side of the light cones becomes vertical at r_+, the event horizon, while their remainder points inwards. Thus the hypersurface r_+ represents the event horizon of the black hole. Analogously, r_- represents an inner horizon of the space-time. Both horizons act as semipermeable membranes, to be passed by light or particles only from the outside to the inside.

The figure also shows, that in region II between the horizons the light cones are always tilted inwards. Thus any object that has passed the outer horizon must inevitably also pass the inner horizon and enter region III. Inside region III, however, the light cones are no longer tilted inwards. Therefore a particle is no longer forced to move towards the singularity, but is free to move inside this region. In fact, only very special geodesics will reach the ring singularity at all.

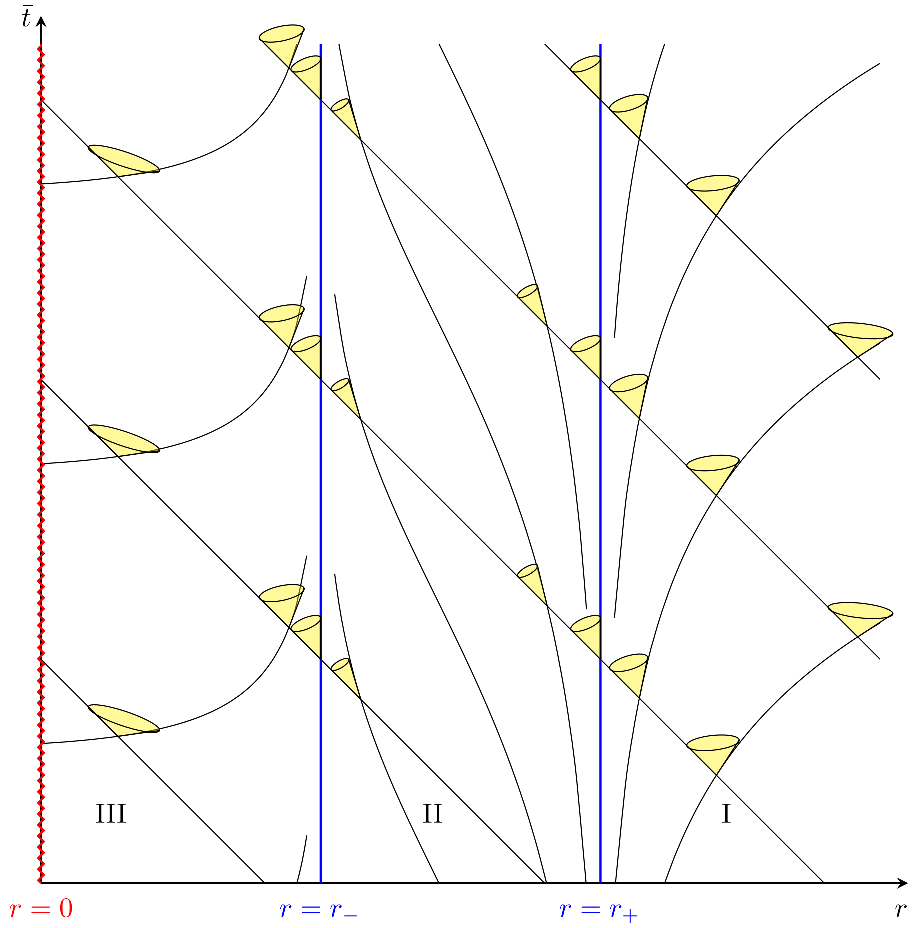

Figure 12. Null geodesics of the Kerr space-time.

3.7. Stationary limit

Now we return to the effects of frame dragging. We consider the motion of light, that is initially tangential to orbits with fixed radial coordinate r and polar coordinate θ. For light, that is initially moving in the same direction as the black hole is rotating, i.e., for co-rotating orbits, we do not expect that anything special might arise. However, we may ask ourselves, whether it will always be possible for light to counter-rotate around the black hole, i.e., follow orbits that move in the direction opposite to the direction of the rotation of the space-time. We know that the rotation of the space-time will drag the light along. So could this drag be able to change the direction of the orbits?

To answer this question we inspect the equations again. In particular, we consider the Lagrangian $\mathcal{L}^*$ for light for fixed radial and polar coordinates. We then find a quadratic equation for $d\phi/dt$. For co-rotating orbits, $d\phi/dt$ is positive, whereas for counter-rotating orbits, $d\phi/dt$ should be negative. We then realize that the angular velocity $d\phi/dt$ changes sign precisely at the hypersurface

$$r^2 - 2mr + a^2 \cos^2\theta = 0. \tag{46}$$

We recognize this hypersurface immediately, since we encountered it before: it is the infinite redshift surface r_{S_+}. Thus outside the surface r_{S_+} light and particles may in principle counter-rotate, but inside the surface r_{S_+} this is no longer possible. The dragging of space-time becomes so strong, that an initially counter-rotating particle will have to change the direction of its orbit in order to co-rotate with the space-time. A sketch of the light cones in the equatorial plane of the space-time in the vicinity of the black hole is seen in figure 13.

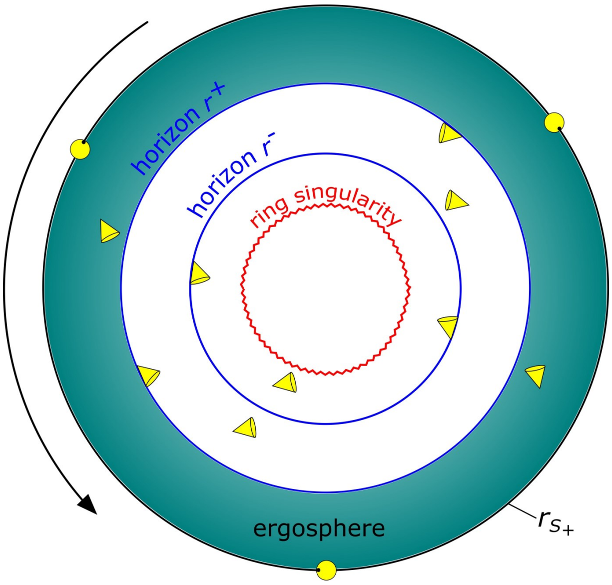

Figure 13. Equatorial plane of the Kerr space-time.

3.8. Ergoregion

We have termed the region between the infinite redshift surface and the outer horizon the ergoregion of the black hole. Besides the interesting fact, that nothing can counter-rotate inside this region, but has to follow the rotational motion of the black hole, this region has another intriguing property. To see this we inspect the effective potential for particle orbits in the space-time. An example is shown in figure 14. The upper curve illustrates the effective potential for co-rotating particles, while the lower curve shows the one for particles that counter-rotate far away, but will be dragged along with the space-time in the ergosphere. Here we note, that negative energies are possible for particles inside the ergosphere.

This fact can be exploited to extract energy from a rotating black hole via the Penrose process [27, 28]. Here one considers a particle that has energy E and is initially counterrotating, i.e., it has negative angular momentum L. This particle enters the ergosphere, where is decays into two particles, one with positive energy E_+ and one with negative energy E_-. Because of energy conservation $E = E_+ + E_-$, and because $E_- < 0$, the energy of the particle with positive energy will be larger than the energy of the orignal particle

$$E_+ = E - E_- > E. \tag{47}$$

The positive energy particle can then leave the ergosphere with an energy greater than the energy of the original particle, while the negative energy particle falls into the black hole. Consequently the black hole loses energy. Maximally 29% of the mass of a rotating black can be extracted by such processes.

3.9. Penrose diagram

Let us now try to extend the Kerr space-time in a similar way as in the Schwarzschild case in order to obtain its maximal extension for the physically most interesting case $m^2 > a^2$, where

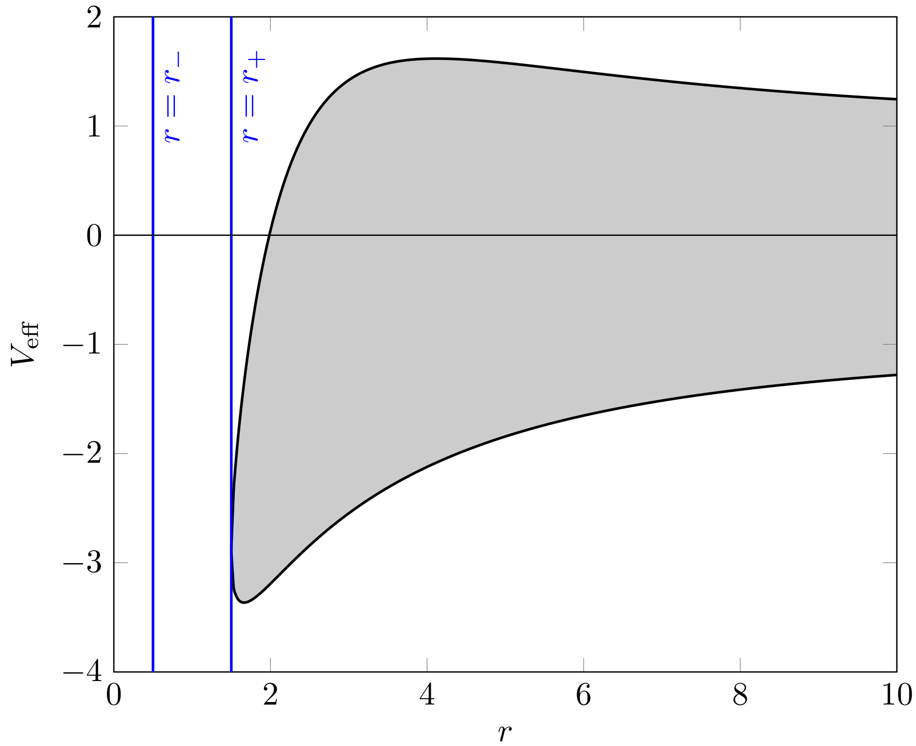

Figure 14. Effective potentials in the Kerr space-time.

we have two horizons $r_\pm$. In the case of the Kerr space-time it turns out, that we have to make an infinite number of transformations, leading to an infinite set of regions. After compactifying the coordinates again, we find the following astounding diagram, that is shown in figure 15.

The coordinates are again chosen such, that the light cones have 45° opening angles, so that the causal structure is evident. The regions I correspond to the outside universe and its infinitely many copies. The regions II represent the region between the outer and inner horizon and its copies. The regions III each contain a ring singularity. But the singularity does not represent a border as in the case of Schwarzschild, where the space-time could not be extended beyond the singularity. Here we can extend the space-time through the disk of the ring, by continuing the radial coordinate r to negative values. Therefore any region III then has an asymptotically flat part and looks similar to the region I in the diagram, except that it hosts a ring singularity.

However, the new part of the region III that is associated with a negative radial coordinate r is physically very different from the region I. In the outer part of region III, where $r < 0$, the universe is antigravitating: gravity is repulsive. We can see this immediately by looking at the corresponding effective potentials in this region. However, we can also guess it from the following simple argument. When we inspect the metric, then there is a single term, which is linear in r, i.e., depends on its sign. This is the term $2mr = 2(-m)|r|$, which we have rewritten in this suggestive way with a minus sign in front of the mass. Since a negative mass would be antigravitating, gravity would be repulsive in a space-time with negative mass.

3.10. No-hair theorem

Now that we have gained a basic understanding of the Kerr space-time let us briefly address another of its intriguing properties, namely that a Kerr black hole has no hair, as Wheeler put it [3]. What is this strange sounding phrase supposed to mean? To answer this question, let

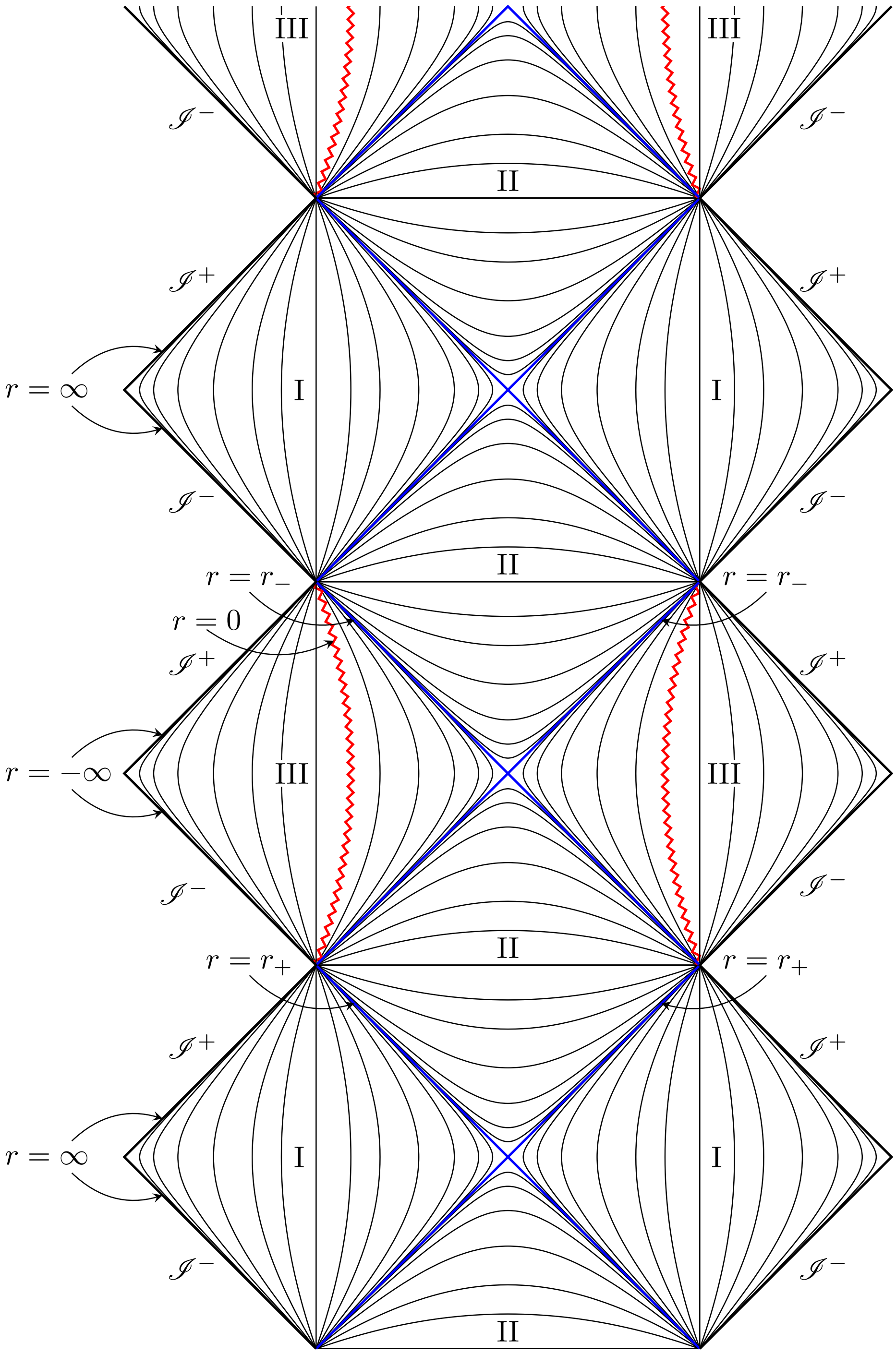

Figure 15. Penrose diagram of the Kerr space-time for $m^2 > a^2$.

us recall, that there are only two numbers that specify the whole Kerr space-time, namely the mass and the angular momentum, when these are known, all is known about the space-time. It is these two global charges, that specify the complete black hole space-time. Of course, one can make a multipole expansion for the space-time and calculate its quadrupole moment, its octupole moment, etc. [29, 30]. However, all these moments can be fully expressed in terms of the mass and the angular momentum. Thus there is no new information entering anywhere. Moreover, it does not matter whatever has formed the black hole. In the end it will only be the mass and the angular momentum that determine the black hole space-time. This has been nicely illustrated by Wheeler in a diagram like figure 16, that has been adapted to my hometown Oldenburg.

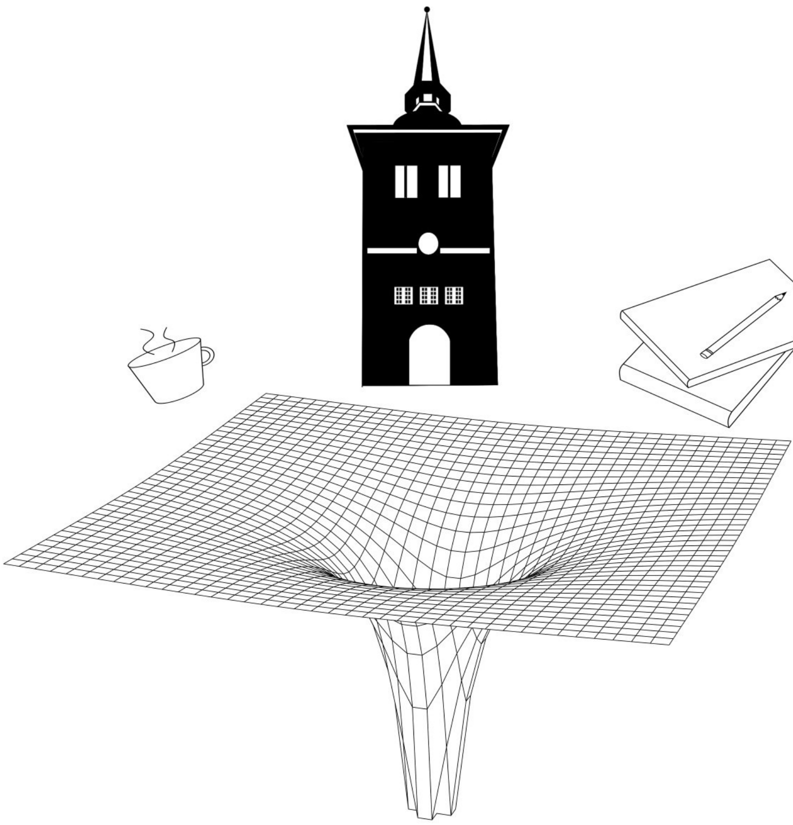

Figure 16. Illustration of the no-hair theorem with the Lappan of Oldenburg.

4. Observations

Certainly the most exciting observations involving black holes in recent times concern the LIGO/VIRGO measurements of gravitational radiation originating from cataclysmic merger events of black holes (see e.g. [31, 32, 33, 34, 35] for the annoucements of the first events). This will, however, not be addressed here, since this thrilling topic is covered by its own set of lectures. Instead we will now focus on the shadow of black holes and the ongoing efforts by the Event Horizon Telescope [36] and Black Hole Cam [37] consortia to observe the shadow of the supermassive black hole at the center of the Milky Way.

4.1. Schwarzschild black hole light ring

We will start by addressing the effective potential of photons for the Schwarzschild metric. This effective potential is illustrated in figure 17. The figure shows, that the effective potential has a maximum, that is located at $r_{\rm ph} = 3m$, i.e., at $3/2$ times the Schwarzschild radius. An extremum of the effective potential shows the location of a circular orbit. But since the extremum is a maximum, this means, that the circular orbit is unstable. This unstable circular orbit is called the light ring.

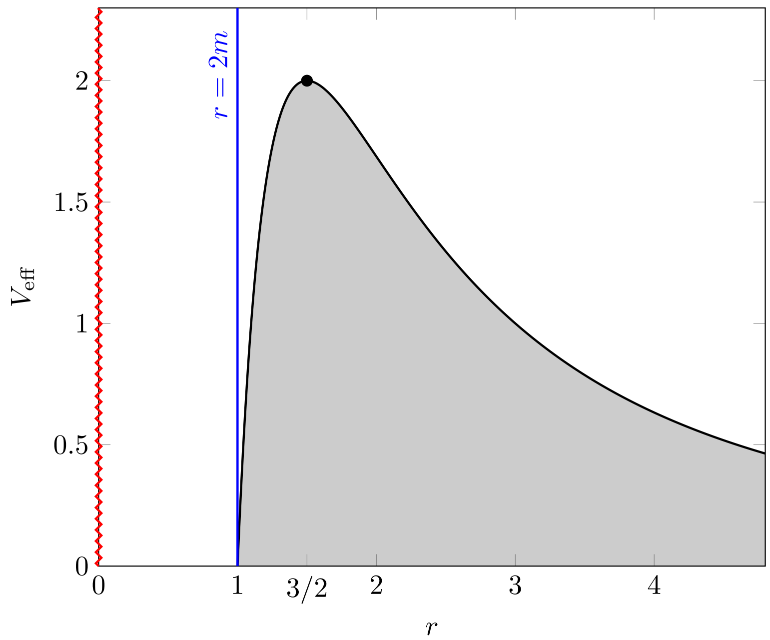

Figure 17. Effective potential for photons in the Schwarzschild space-time.

Its presence reveals, that when undisturbed, light could in principle orbit indefinitely on the sphere that is specified by the radial coordinate of the light ring. This sphere is therefore also called the photon sphere. Because of the instability, however, light will either leave the sphere towards the outside universe or towards the black hole.

4.2. Schwarzschild black hole shadow

If we assume that no light is emitted from the region between the horizon and the photon sphere, then any light that will reach this region will come from sources residing outside the photon sphere. Depending on its impact parameter, this light will either fall into the black hole, or it will be reflected outwards. But any light that will reach the region between the photon sphere and the horizon will irrevocably be lost. Since no light will escape from that region to the outside, this region will appear dark. Therefore it has been named the black hole shadow.

For the Schwarzschild black hole the angular size of the shadow has first been calculated by Synge [38]. To follow his reasoning let us consider figure 18. This shows the circumference of the horizon and the photon sphere with radial coordinates $2m$ and $3m$, respectively, and the angle α as seen by an observer located further away from the black hole as specified by the value of the radial coordinate r_{O}. To obtain the angle α we need to take into account, that the space-time is curved. The radial distance is not given by the radial coordinate r, which only describes the circumferential radius. Instead we should employ the Schwarzschild line element to calculate the radial distance via $d\bar{r} = \sqrt{g_{rr}}dr$. Therefore the angle α is given by

$$\cot\alpha = \frac{d\bar{r}}{rd\phi} = \frac{1}{r\sqrt{1-2m/r}}\frac{dr}{d\phi}. \tag{48}$$

The expression for $dr/d\phi$ is known from the equations of motion in the Schwarzschild space-time and can therefore be inserted to yield

$$\cot^2\alpha = \frac{1}{\left(\frac{r}{2m}-1\right)}\left(1-\frac{r}{3m}\right)^2\left(1+\frac{r}{6m}\right). \tag{49}$$

Massaging this formula a little and employing for the observer the coordinate $\rho_{\rm O} = r/(2m)$ leads to the final expression for the angle determining the size of the shadow of a Schwarzschild black hole

$$\sin^2\alpha = \frac{27}{4}\,\frac{(\rho_{\rm O}-1)}{\rho_{\rm O}^3}. \tag{50}$$

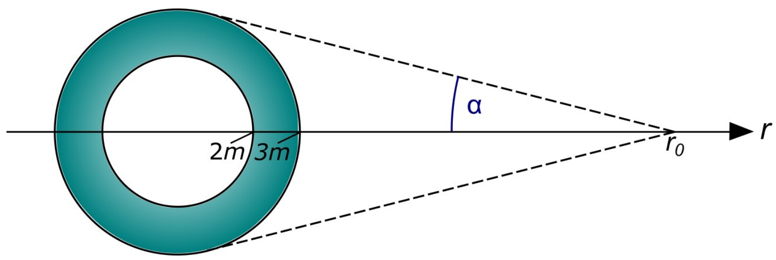

Figure 18. Sketch to find the angular size of the black hole shadow in the Schwarzschild space-time.

4.3. Kerr black hole shadow

Of much more relevance should be the shadow of a rotating black hole. This shadow will no longer look spherically symmetric, unless viewed from the direction of the rotation axis. To obtain its shape one has to consider, that there will be co-rotating and counter-rotating light rays, and one has to find the photon region for the full set of light rays, i.e., the region where unstable spherical paths are possible.

When the angular momentum of the black hole is increased the shadow changes its shape from a spherical shape to a deformed shape with an asymmetry, that arises due to the different behavior of co-rotating and counter-rotating light rays. The calculations, as first done by Bardeen [39] show, that this asymmetry increases with increasing specific angular momentum, until the highly asymmetric shadow of an extremal black hole is obtained. The dependence of the shape on the specific angular momentum is shown in figure 19 [40].

*4.4. Sagittarius A**

A simple estimate of the size of the shadow of the black hole at the center of the Milky Way is obtained by employing the distance from Earth of about 26.000 light years and a mass of about 4.3 million $M_\odot$. This yields an angular size on the order of 50 μas. In order to measure such extemely small angular sizes, that are sometimes compared to observing a grapefruit on the surface of the moon, the EHT and the BlackHoleCam consortia use interferometry with telescopes based around the globe, to provide an enourmous baseline and thus the needed tremendous resolution. While no images of the shadow have been published so far, there are numerous simulations available, based on highly advanced theoretical modelling. It will be exciting to find out how the shadow really looks like, and whether it has any similarities with the beautiful shadow of the black hole Gargantua of the movie Interstellar as sketched in Fig. 20.

As beautifully explained in Thorne's book on the science of Interstellar [41], the figure shows besides the dark shadow of the black hole the bright accretion disk. In particular, what we

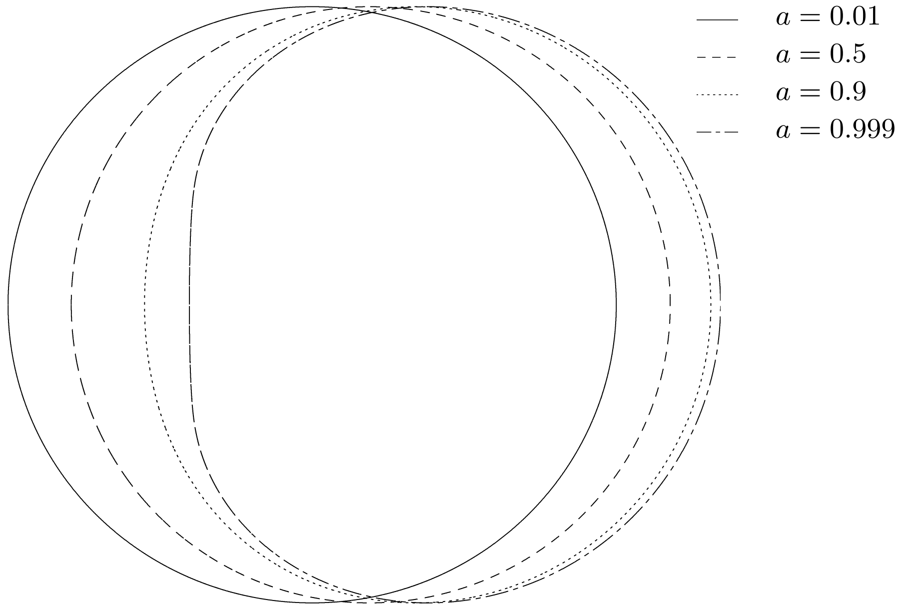

Figure 19. Contours of shadows of Kerr black holes for several specific angular momenta as seen from the equatorial plane.

see in front of the black hole is light that orginates from the part of the accretion disk that is located on the front side of the black hole. The part of the accretion disk that we see above the black hole corresponds to light, that originates from the back side of the accretion disk behind the black hole. It is the effect of the very strong bending of light in the vicinity of the black hole, that makes it visible to us. Similarly, the part of the accretion disk that we see below the black hole originates from the back side of the black hole, but in fact from the lower side of the accretion disk there. Together they form this beautiful picture of the black hole shadow surrounded by its accretion disk.

5. Conclusions

Black holes are beautiful mathematical and highly fascinating astrophysical objects. They have made their appearance first in Einstein's GR, and it has taken a long time before the physical meaning of these solutions could be fully understood. But once their characteristic features became clear, their presence in the universe was expected, and soon numerous promising black hole candidates could be identified in the heavens.

Besides the stellar black holes it is the supermassive black holes lurking at the center of galaxies, that have attracted much attention, captivating the minds of physicists and laypersons alike. While it represents an intriguing puzzle, how such giants could have evolved so very early in the evolution of the universe as observations tell, lifting the veil of the mysteries, that enshroud these gargantuan awesome entities, will contribute enormously to our understanding of nature.

A foremost avenue here is the study of astroparticle physics, since highly energetic particles should have been sent towards us since eons, originating in active galactic centers that represent the environments of such supermassive black holes. An impressive such case at hand was announced last summer: the neutrino event IceCube-170922A that is associated with the blazar TXS 0506+056 [42].

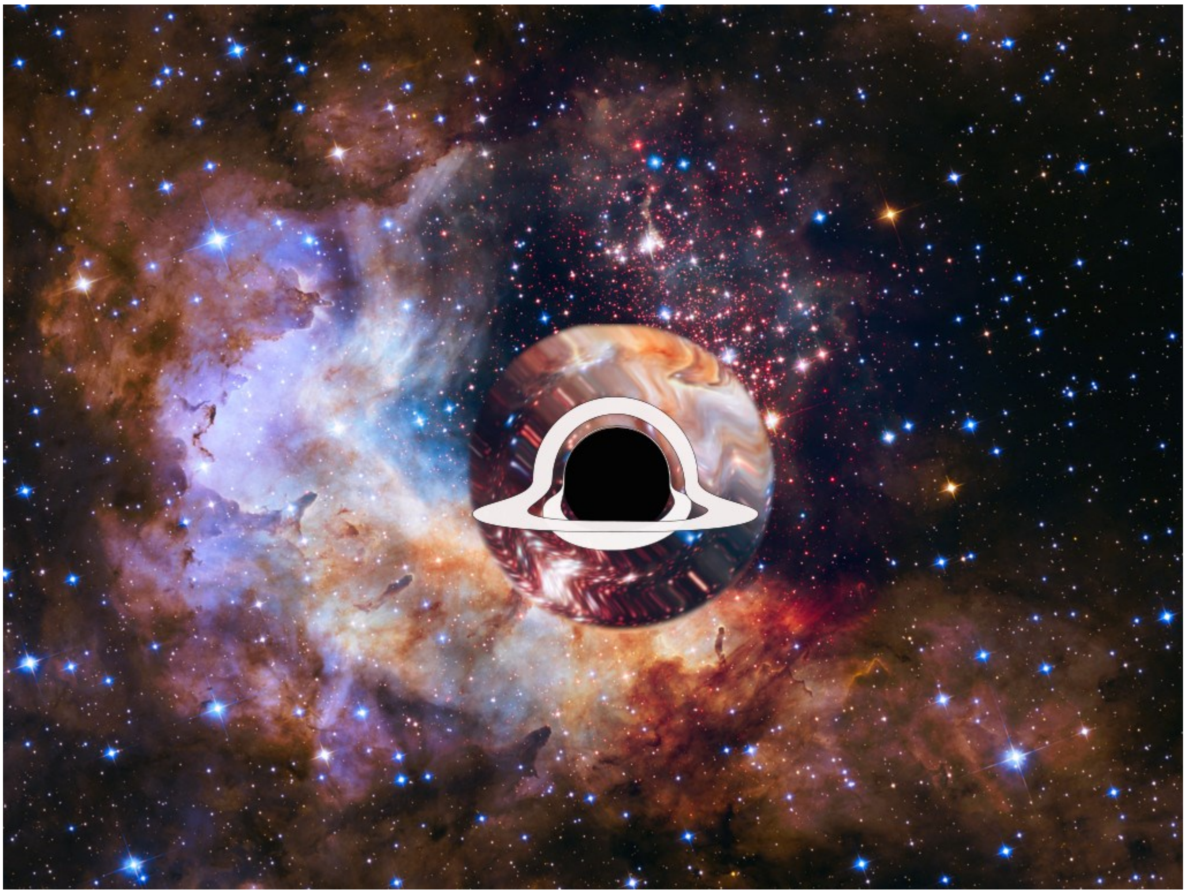

Figure 20. An artist's view of a black hole surrounded by an accretion disk as seen by a nearby observer.

Acknowledgments

J.K. would like to acknowledge support by the DFG Research Training Group 1620 *Models of Gravity* and the COST Action CA16104 *GWverse*. She would also like to thank Jens Drawer and Theresa Ott, for the preparation of numerous figures.

References

[1] Weinberg S 2018 *Phys. Rev. Lett.* **121**, 220001
[2] Weinberg S 1972 *Gravitation and Cosmology: Principles and Applications of the General Theory of Relativity* (New York: John Wiley & Sons)
[3] Misner C W, Thorne K S and Wheeler J A 1973 *Gravitation* (San Francisco: Freeman)
[4] d'Inverno R 1992 *Introducing Einstein's relativity* (Oxford: Clarendon)
[5] Hobson M P, Efstathiou G P and Lasenby A N 2006 *General relativity: An introduction for physicists* (Cambridge: University Press)
[6] Schutz B 2009 *A First Course in General Relativity* (Cambridge: University Press)
[7] Carroll S 2014 *Spacetime and Geometry: An Introduction to General Relativity* (Harlow: Pearson)
[8] Frolov V P and Zelnikov A 2015 *Introduction to Black Hole Physics* (Oxford: University Press)
[9] Schwarzschild K 1916 *Sitzungsber. Preuss. Akad. Wiss. Berlin (Math. Phys.)* **1916**, 189
[10] Kiefer C 2006 *Annalen Phys.* **15**, 129
[11] Zeldovich Ya B and Novikov I D 1971 *Relativistic Astrophysics: Stars and Relativity, Volume 1* (Chicago: University of Chicago Press)
[12] Greenstein G 1985 *Frozen Star: of Pulsars, Black Holes and the Fate of Stars* (New York: Plume)
[13] Shipman H L 1975 *Astrophys. Lett.* **16**, 9

[14] Lewin W and van der Klis M 2006 *Compact Stellar X-ray Sources* (Cambridge: University Press)
[15] Kormendy J and Richstone D 1995 *Ann. Rev. Astron. Astrophys.* **33**, 581
[16] Magorrian J *et al.* 1998 *Astron. J.* **115**, 2285
[17] Ghez A M *et al.* 2008 *Astrophys. J.* **689**, 1044
[18] Genzel R, Eisenhauer F and Gillessen S 2010 *Rev. Mod. Phys.* **82** 3121
[19] Johannsen T 2016 *Class. Quant. Grav.* **33**, 113001
[20] Abuter R *et al.* [GRAVITY Collaboration] 2018 *Astron. Astrophys.* **615**, L15
[21] Kerr R P 1963 *Phys. Rev. Lett.* **11**, 237
[22] Kerr R P and Schild A 2009 *Gen. Rel. Grav.* **41**, 2485
[23] Bardeen J M 1970 *Nature* **226**, 64
[24] Penrose R 1969 *Riv. Nuovo Cim.* **1**, 252 [2002 *Gen. Rel. Grav.* **34**, 1141]
[25] Wald R M in Iyer B R (ed.) et al. 1999 *Black holes, gravitational radiation and the universe* (Dordrecht: Springer)
[26] Carter B 1968 *Phys. Rev.* **174**, 1559
[27] Penrose R and Floyd R M 1971 *Nature* **229**, 177
[28] Bardeen J M, Press W H and Teukolsky S A 1972 *Astrophys. J.* **178**, 347
[29] Geroch R P 1970 *J. Math. Phys.* **11**, 2580
[30] Hansen R O 1974 *J. Math. Phys.* **15**, 46
[31] Abbott B P *et al.* 2016 *Phys. Rev. Lett.* **116**, 061102
[32] Abbott B P *et al.* 2016 *Phys. Rev. Lett.* **116**, 241103
[33] Abbott B P *et al.* 2017 *Phys. Rev. Lett.* **119**, 141101
[34] Abbott B P *et al.* 2017 *Phys. Rev. Lett.* **118**, 221101
[35] Abbott B P *et al.* 2017 *Astrophys. J.* **851**, L35
[36] https://eventhorizontelescope.org/
[37] https://blackholecam.org/
[38] Synge J L 1966 *Mon. Not. Roy. Astron. Soc.* **131**, 463
[39] Bardeen J M in *Black Holes*, DeWitt C and DeWitt B S (eds.) 1973 (New York: Gordon and Breach)
[40] Cunha P V P, Herdeiro C A R, Radu E and Runarsson H F 2016 *Int. J. Mod. Phys.* D **25**, 1641021
[41] Thorne K S 2014 *The Science of Interstellar* (New York: Norton & Company)
[42] Aartsen M G *et al.* [IceCube Collaboration] 2018 *Science* **361**, 147